Chapter 1

Design and implementation of trigger algorithms in single photon counting systems

In this chapter the work carried out to develop Data Acquisition systems for detectors using the Single Photon Counting Technique with emphasis on the GAW project is presented. More specifically, the work on the trigger system and the development of firmware for the GAW electronics is reported.

1.1 Single photon counting systems

Single Photon Counting (SPC) is a well-established technique for the detection of very faint light levels [9]. For faint light levels, photons arrive individually to the photocathode of the PMT. For each photon a voltage pulse will be produced by the amplification chain of the PMT. Therefore, in the photon counting mode, individual pulses can be detected using a simple threshold. The number of detected pulses is an estimator of the light arriving to the PMT.

The front-end electronics based on the SPC technique is very simple and usually makes use of amplifiers and comparators to transform analog signal pulses into digital pulses by setting a threshold. This technique is very effective [1] in terms of stability, detection efficiency and signal to noise ratio, on the condition that pulses are properly resolved within the maximum frequency of the system. Unlike the charge collection technique, in which the analog signal is digitalised, there is no information about the amplitude of each signal. Consequently if several signal pulses arrive within the time resolution of the system they will pile-up and the system will

only count one photon. The phenomenon is usually named photon pile-up and is related to the saturation of the system.

The SPC technique is suitable for the instrumentation of the focal surface of a detector if the signal will not produce pile-up. This can be achieved by lowering the pixel size, and thus increasing the number of pixels, and by increasing the acquisition frequency. The use of such simple electronics allows the use of a very high number of acquisition channels with very good time resolution.

The triggering system of such detectors using the SPC technique are usually implemented with several levels. The first trigger level can be considered as the threshold applied to the analog signal. Higher trigger levels include the definition of a minimum number of detected photons at a given pixel, and algorithms that analyse the characteristics of the signal. The top level triggers analyse the pattern produced in the pixels, the number of photons detected, and its evolution in time allowing the elimination of the random and uncorrelated background events.

An analog acquisition system, with the same performance, would increase the information collected and thus represent a better DAQ system. Such system could be implemented using an integration ADC with a small gate defined from a fast threshold, by a flash ADC running at high frequency or by a peak-sensing ADC. However such solutions represent an enormous increase in the price and power consumption per channel. The design of an acquisition system will have to make a trade-off between the acquired information per channel and the number of acquisition channels. The performance of similar Imaging Atmospheric Cherenkov telescope layouts, using different approaches for the front-end electronics, has been studied and compared at the level of the trigger efficiencies and energy thresholds in [6]. The results obtained clearly favours the option for a focal surface with high pixelisation using the Single Photon Counting technique.

The Single Photon Counting Technique was adopted for the EUSO detector. EUSO is basically an UV telescope with a highly pixelated focal surface and aims to detect the fluorescence light from cosmic rays showers in the Earth's atmosphere. The high number of channels, the low light level produced by cosmic rays and the constraints imposed to space based experiments in terms of power, weight and telemetry led EUSO to adopt the Single Photon Counting Technique for the instrumentation of its focal surface.

In the focal surface of EUSO an Extensive Air Shower is imaged as a spot whose intensity and position evolves with time producing a track. High-energy shower events are clearly distinguishable from the background and a simple signal persistency trigger can be used. For lower energy events ($< 10^{20}$ eV) the signal to noise

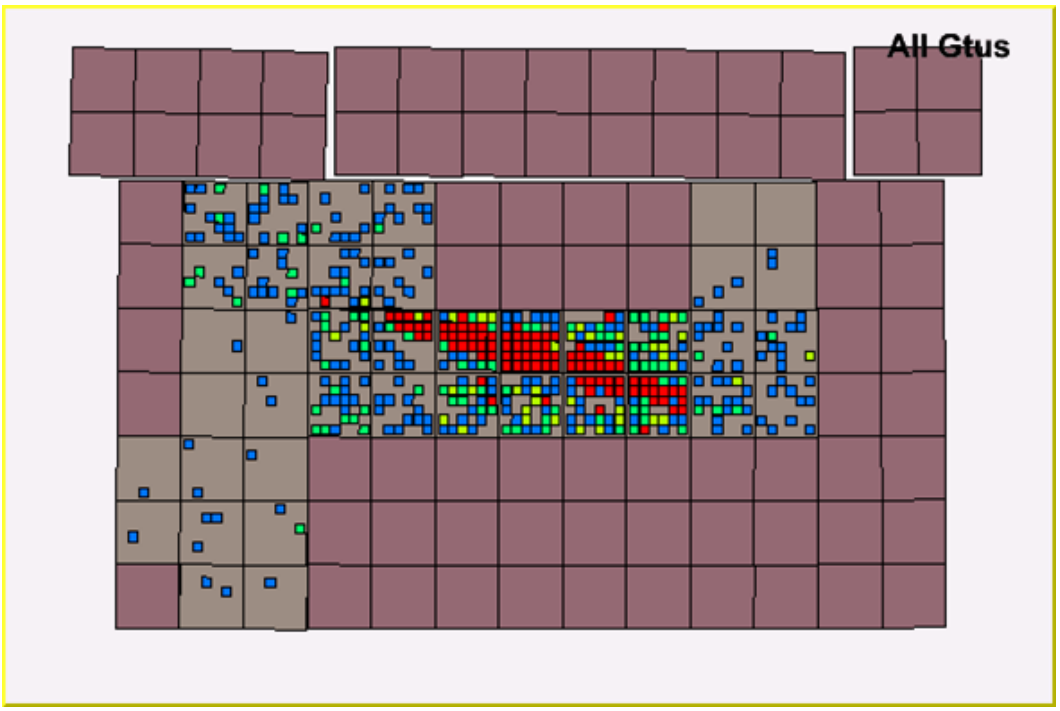

Figure 1.1: Simulated Shower in ESAF. Each big square represents a MAPMT while the small pixels represent the pixels. Active pixels are presented in colour which represents the number of collected photons.

ratio is reduced and the detection of the signal must rely on the identification of its properties, namely the space-time patterns, that differ a lot between events and background.

The EUSO trigger has been designed to provide a good discrimination of shower events from the background for energies as low as possible ($\sim 5 \cdot 10^{19}$ eV). An analog threshold is used for the definition of the single photon pulses. The pulses are counted in a time window and a digital threshold is used to define an active pixel. The second trigger level is a contiguity trigger that identifies the pattern of a cosmic ray in the focal surface of EUSO. The trigger is performed online and searches for a continuity of a line in time. This is done by searching if in consequent time frames there are adjacent pixels with signal. Such a scheme can be implemented using very simple electronics. The triggering system is described in detail in [5].

The triggering system simulation was firstly studied using IDL at Palermo [5]. It was implemented in the Euso Simulation and Analysis Framework (ESAF)[11, 14] at Lisbon and a first validation of the simulation was performed and reported [4]. Figure 1.1 represents a simulated shower using ESAF that met the trigger condition as implemented in the simulation. In the context of the study of cosmic ray space detectors, the performance of the detector was assessed, using ESAF, in more detail

in [13].

Unfortunately external conditions prevented EUSO to advance to the phase B of the project, although phase A was concluded successfully. During phase B the detector system was to be refined and the concrete implementation of its electronics system designed. The triggering system was to be studied more in depth, its parameters fine tuned and its implementation designed taking into account the constraints imposed by the electronics system foreseen.

The same approach of EUSO was applied in the context of an Imaging Atmospheric Cherenkov Telescope with large Field of View capability - the Gamma Air Watch (GAW) project. The DAQ and triggering system of the telescope, where the LIP group has taken particular responsibilities, will be discussed in the following section.

1.2 Data acquisition and trigger in the GAW experiment

GAW, described in section **??**, is a wide field of view Imaging Atmospheric Cherenkov Telescope. GAW uses an innovative approach for the collection of Cherenkov light generated by EAS, in particular the Single Photon Counting Technique to acquire light signals.

1.2.1 Requirements

The GAW electronics has been designed to fully match the specific requirements imposed by the new proposed approach. A large number of active channels constitute the focal surface of the GAW telescope making it basically a large UV sensitive digital camera with high sensitivity and time resolution. The GAW electronics design is based on single photoelectron counting method [6](front-end) and free running method (data taking and read-out)

1.2.2 Electronics Layout

GAW Focal Surface Detector, represented in figure 1.2, is formed by an array of Multi-Anode Photo Multipliers (MAPMTs) coupled with the electronic instrumentation, UVIScope (Ultra Violet Imaging Scope), capable of conditioning, acquiring and processing, at a high rate, a large number of high speed pulse signals.

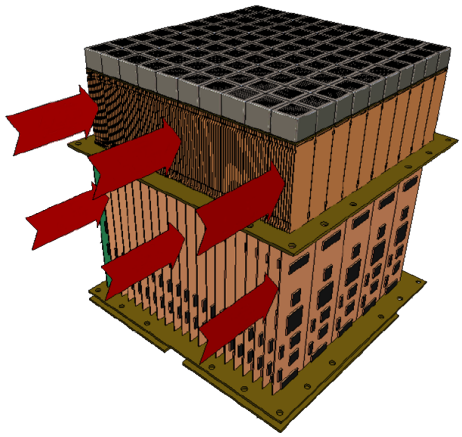

Figure 1.2: Artist view of the GAW Focal surface

The UVIScope is built as a modular system, the elementary unit being a Macrocell. The Macrocell, represented in figure 1.3, is composed by four MAPMT, four FEBrick units, four ProDAcq and HV, LV and control boards. At the bottom of each Macrocell we can find a Trigger board. Each Macrocell unit can operate independently. A simplified scheme of a Macrocell unit is shown in figure 1.3. When inserted in the UVIScope the Trigger boards communicate with the adjacent ones and the control boards communicate with an external control board. The configuration, monitoring and read-out of the system will be performed through the external control board. The Macrocells will be mounted in a mechanical structure coupled to the Telescope body. In figure 1.4 it is represented the focal surface in its mechanical structure for the phase I (a) and phase II (b) of the project.

In the Phase I, a reduced focal surface, composed by 8 $\times$ 8 MAPMTs, will be used, covering a FOV of 6° $\times$ 6°. During this phase it is foreseen that the focal surface will be moved to different positions in order to test the performance of the telescope at off-axis angles up to 12°.

In the Phase II the whole focal surface will be covered by 1600 PMTs, arranged in a grid of 40 $\times$ 40, providing a field of view of 24° $\times$ 24°. In order to minimise the effect of the optical aberrations the Macrocells height will be adjusted so that the MAPMT array will follow, as close as possible, the curvature of the ideal focal surface, as can be seen in figure 1.4(b).

MAPMT

The MAPMT used for GAW Focal Surface Detector is the Hamamatsu mod. R7600-03-M64 with 64 anodes arranged in an 8×8 matrix. The physical dimension of the

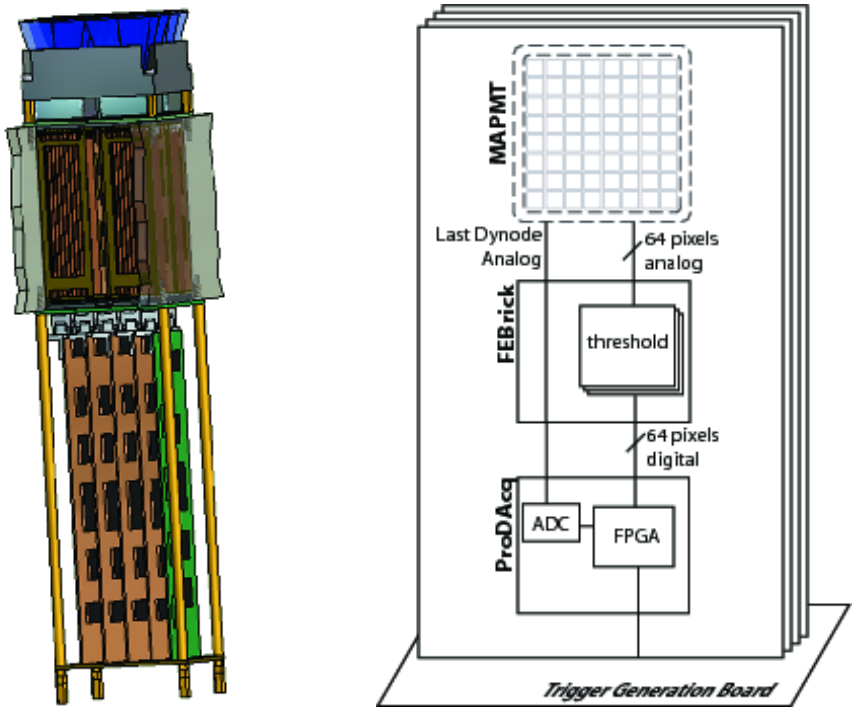

Figure 1.3: GAW Macrocell. Left: Artist view. Right: Simplified scheme

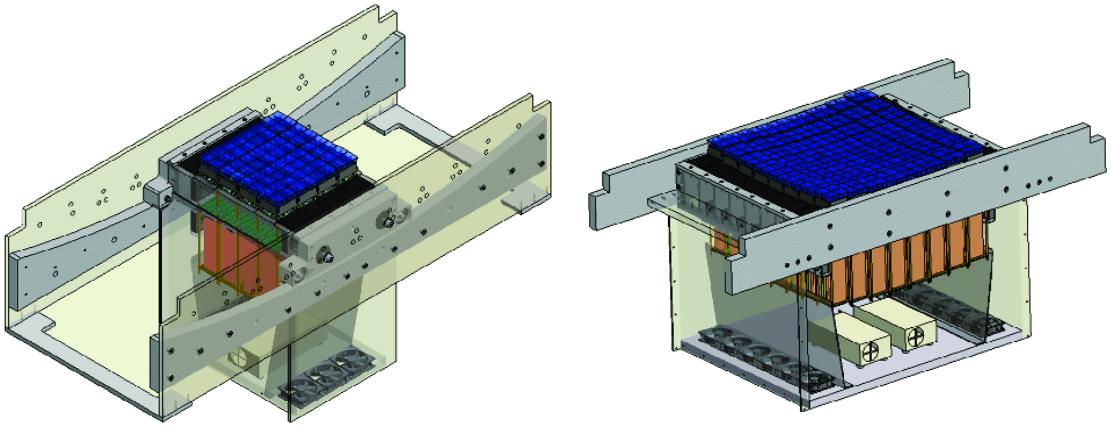

(a) Phase I (b) Phase II

Figure 1.4: GAW Focal Surface

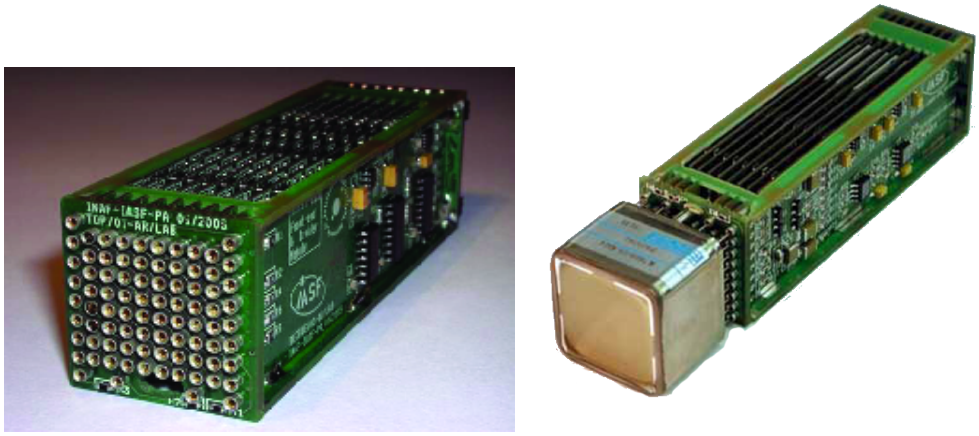

(a) with socket visible (b) with PMT installed

Figure 1.5: Photographs of a FEBrick unit.

tube section is $25.7 \times 25.7\,\mathrm{mm}^2$ (minimum true area is $18.1 \times 18.1\,\mathrm{mm}^2$), with length of approximately 33 mm and weight of 30 g. Each pixel has a size of 2×2 mm separated by a pitch of 0.3 mm. The crosstalk between pixels is 2 % and the anode dark current is 0.2 nA. The Phototube has a transit time of 10.9 ns with a spread of 0.3 ns. The output signal has a rise time of 1 ns. The tube is equipped with a bialkali photocathode and a 0.8 mm thick UV-transmitting window, ensuring good quantum efficiency for wavelengths longer than 300 nm, with a peak of 20% at 420 nm. The device has a Metal Channel Dynode structure with 12 stages, providing a gain of the order of $3 \cdot 10^5$ for a 0.8 kV applied voltage.

FEBrick

The front-end electronics of GAW is realised in a modular way. The blocks that compose the Front-End are called the Front-End Brick - FEBrick (Figure 1.5). The FEBrick is designed for a single MAPMT, implementing the front-end electronics for 64 anodic channels, working in single photon counting mode, and the last dynode signal that will be acquired as a high speed integration channel. The FEBrick also provides the HV power supply to the MAPMT and monitors the temperature.

The FEBrick develops on axis along the bottom of the MAPMT as an appendix of identical section ($25.7 \times 25.7\,\mathrm{mm}^2$) with a length of ~ 85 mm, that allows placing units side by side. Each FEBrick unit is connected, through a socket visible in figure 1.5(a), to the bottom of the MAPMT. In this way, the MAPMT is placed in a close contact with the input of the amplification channels in order to preserve the anodic signals.

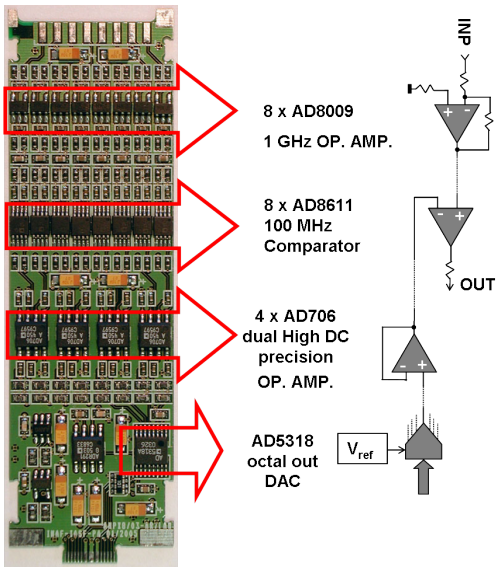

Figure 1.6: A module of the FEBrick showing the front-end scheme for an anodic channel.

A FEBrick is composed of 8 parallel boards, each implementing the electronics for a line of 8 pixels of the MAPMT. Figure 1.6 represents one of these boards and the chain of the front-end electronics for each anodic channel. Each channel is composed by a fast amplifier and a 7 ns accuracy discriminator channel for Single Photon Detection. The amplification channel is equipped with an amplifier of 1 GHz bandwidth, at unitary gain, and 5500 V/μs slew rate. The amplifier gain is set to $G = 10$ (obtaining a 320 MHz bandwidth) to increase sensitivity and detect very small signals. The discrimination is performed using a comparator with 100 MHz input frequency and 4ns propagation delay. The reference voltage of the comparator, that acts like the discrimination level, is generated by a 12 bit DAC and ranges from 0 to +250 mV in $\sim$ 60 μV steps. The discrimination level for each channel is set individually to make it possible to equalise input offset voltage differences between the discriminators and gain differences between the 64 anodes.

On the lateral sides of the FEBrick there are two boards in which the High Voltage Power Supply, the last dynode Front-End electronics and the Front-End management are implemented.

The Front-End electronics for the dynodic channel, operating as charge integrator, is equipped with a FET amplifier of 145 MHz bandwidth at unitary gain, 180 V/μs slew rate and 2 pA input bias current.

The FEBrick provides also the HV power supply to the MAPMT through a low power active high voltage divider. Two separate high voltage lines are provided:

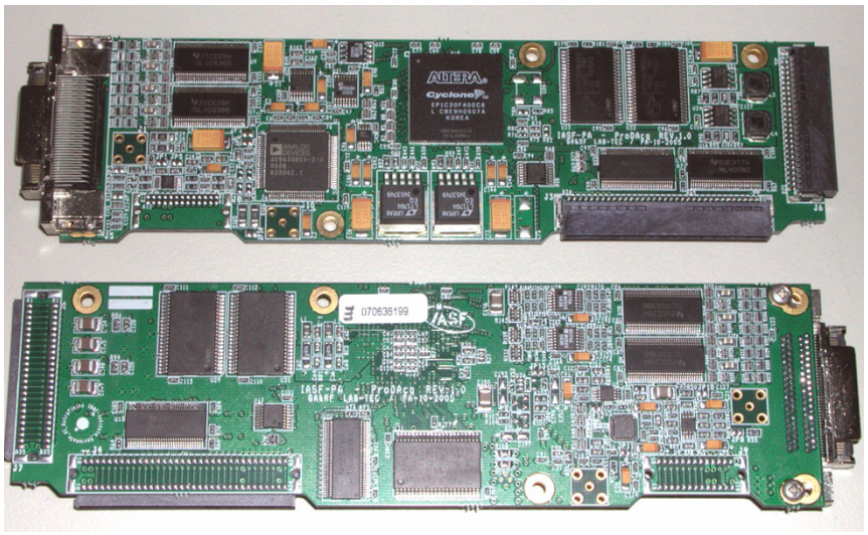

Figure 1.7: The ProDAcq Board

the first line supplies directly the last dynode and the second one supply the other dynodes through a low power active divider.

A temperature sensor detects FEBrick unit average temperature and outputs a direct digital value to provide thermal conditioning management. The temperature sensor can operate in the range of -35 to $+85$°C with an accuracy of ± 1°C.

The FEBrick power consumption is about 10 W. A side-by-side assembling of many FEBrick units should need adequate thermal conditioning.

All FEBrick units, required for the whole focal surface, are placed together on the top of a backplane while on the bottom are placed the ProDAcq units. Backplane is in charge to connect FEBrick unit signals to the relevant ProDAcq units.

ProDAcq

The ProDAcq (figure 1.7) unit is internally managed by a reprogrammable FPGA. Figure 1.8 shows a simplified scheme of the ProDAcq, its operation and relation with the other components of the system. The ProDAcq samples the digital information from the 64 anodic channels with a frequency of 100 MHz and calculates the number of pixel-on. This information is then passed-on to the associated Trigger Generation board. Upon receiving a Trigger Strobe from the Trigger Generation board, the ProDAcq saves the event information in a memory. Digital signals are recorded inside three memory banks for 192 Kword storage capacities.

The ProDAcq is also responsible for the digitisation of the last dynode analog signal through two ADCs that sample the signal, one with a sampling frequency of 80 MHz and a resolution of 14 bits, the other with a higher acquisition rate of

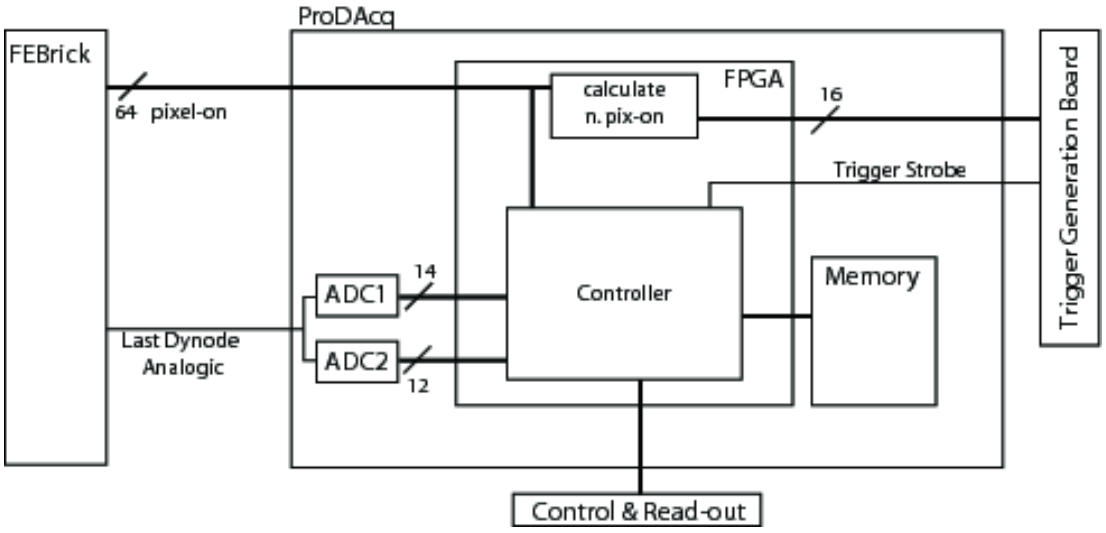

Figure 1.8: Simplified scheme of the ProDAcq board, its operation and relation with the other components of the system.

210MSPS but a lower resolution of 12bits. In this way, the input analogue signal may be sampled at high speed or with high accuracy, according to the wiring combination of two ADC converters.

The ProDAcq units also sample an internal temperature sensor, signal alarm conditions and allow access to the event memory for the read-out of triggered events. The ProDAcq will also register the sky image seen by the PMT pixels, which is recorded as the number of counts in each second for each pixel.

ProDAcq units are inserted on the bottom of the backplane through which the signals of the relevant FEBrick units are received and are terminated on a Trigger Generation Board equipped with Trigger and Timing Synchronisation devices, instrumentation management, power supply and external host interface.

Trigger Generation Board

The trigger generation board is responsible for the generation of local trigger signals. The DAQ system of GAW has an array of these boards, each connected directly to four (2×2) ProDAcq boards and to their neighbours. Trigger generation boards are composed, basically, by an FPGA that receives the number of active pixels from four ProDAcqs, receives and sends data to their neighbours and evaluates if the trigger conditions are met for the set of information available. If the condition is met the board will issue a trigger signal that, when validated, will cause the ProDAcq boards to save the event information for later retrieval.

1.2.3 Trigger system concept

The main requirement of the GAW trigger system is to be able to have a good efficiency at the lowest possible energy, keeping a high rejection power of the background, dominated by the Night Sky Background (NSB).

The Cherenkov signal will produce an image in the camera that adds up to the background. Since the focal surface is highly pixelated this excess light is translated directly into an excess of the number of activated pixels. The GAW triggering system relies on the detection of an increase in the number of activated pixels in a region of the focal surface. More specifically the system is a majority trigger that will search for, at least, a defined number of activated pixels in a square of $k \times k$ pixels.

The noise counting rate, n, of each telescope can be calculated knowing the average value of the background and applying the optical and geometrical characteristic quantities of the telescope. For an individual pixel n is then calculated as

$$n = \langle B \rangle \cdot A \cdot \Omega_{pix} \cdot \Delta t \cdot \varepsilon_{total}$$

where $\langle B \rangle$ is the average value of the Night Sky Background, A is the collecting area of the telescope, Ω_{pix} is the solid angle subtended by one pixel, Δt is the time interval of a Gate Time Unit (GTU) and ε_{total}, the global efficiency of the telescope. The option for a highly pixelized focal surface running at a high acquisition rate (100 MHz) makes the pixel solid angle and the Gate Time Unit (GTU) small, thus minimising the noise in each pixel.

The average value of the Night Sky Background was measured [7] at the Calar Alto Observatory and its rate is estimated by

$$\langle B \rangle = 2200\,\text{photons} \cdot \text{m}^{-2}\text{ns}^{-1}\text{sr}^{-1}$$

For GAW $A = 3.5\,\text{m}^2$, $\Omega_{pix} = 2.3 \times 10^{-6}$ sr, $\Delta t = 10$ ns and $\varepsilon_{total} = 0.06$[7]. With these parameters the mean noise counting rate, per pixel, is estimated to be $n \sim 0.01$ photoelectrons/pixel/GTU. The number of photoelectrons in each pixel and in each GTU then fluctuates according to a Poissonian distribution with a mean value of 0.01.

The Cherenkov signal is an intense and fast light pulse which produces an increase, during a short time (< 10 ns), in the number of pixels with signal in a small region of the focal surface ($0.5° \times 1°$). The concept of the GAW trigger system is to search, online, the whole focal surface for an increase in the number of pixels-on in predefined regions large enough for the signal to be contained inside.

1.2.4 Trigger system design

The GAW trigger system is designed to work in three levels. The first trigger level defines a pixel-on. The second trigger level searches the focal surface for an increase of pixels with signal. The third trigger level validates the second level triggers and signals the region of interest of the focal surface to be read. Each level is implemented in different parts of the GAW DAQ electronics described previously.

First Trigger Level

At the first trigger level the signals from the PMT pixels are subjected to a simple threshold and are transformed into digital signals. A pixel-on is defined here as a pixel which has a signal greater than the set threshold.

The first trigger level is implemented on the front-end electronics (FEBrick), namely as a fast discriminator. The specific detail of the electronics of this trigger is described in 1.2.2.

The thresholds are set independently for each front-end channel, taking into account differences in gain and amplification. The threshold is set below the single electron response of the pixel and above the electronics noise of the amplification chain, initially in the laboratory and are afterwards adjusted on site by means of a calibration run of the telescope.

After this first trigger level, the signal recorded in each of the 64 pixels of one PMT is transformed into 64 logic signals indicating the pixels that have signal. This information is passed directly to the second trigger level.

Second Trigger Level

The second trigger level, the core of the trigger system, searches for an excess in the number of pixels-on. This trigger level scans the digital information received from the first trigger level and searches the focal surface, online, for a given number of pixel-on inside all possible trigger-cells (squares of 2×2 PMTs). The second level trigger is digital and as such can be implemented in FPGAs. Due to its complexity and high number of channels involved, it is implemented in the ProDAcq boards and in the Trigger Generation boards.

The FPGA in the ProDAcq board receives digital information about the individual state of the 64 anode channels of the associated MAPMT and calculates the total number of pixel-on which is then passed to the Trigger Generation board to which the ProDAcq is connected to.

Each Trigger Generation board receives the number of Pixel-on from four ProDAcqs and is connected to their neighbour trigger generator board so that information essential for the generation of a local Second Level Trigger can be shared.

The trigger algorithm, implemented in the FPGAs of the Trigger Generation boards, works online in a pipeline with three steps. On the first step, each FPGA receives the number of Pixel-on from the four ProDAcq attached to it. On the second step it transmits information about relevant PMTs to its neighbour FPGAs on the right and on the bottom, receiving data from the top and left neighbours. This communication scheme allows for each FPGA to have access to the number of pixel-on for a set of 3×3 PMTS. On the third step each FPGA will search for a number of pixel-on greater than a programmable value in all possible trigger-cells with the information available to that FPGA. If this condition is met a second level trigger is generated and passed to the third trigger level. With this scheme implemented the whole focal surface can be searched for the trigger-cells that meet the trigger condition.

The timing for the triggering system is critical. Since the chain of operations must always take the same predetermined time so that the pipeline can work and the triggering data can be recovered from memory and saved.

Figure 1.9 represents this trigger scheme with an example of a focal surface of 6×6 MAPMTs. This corresponds to having a grid of 3×3 Trigger Generation Boards. The first step of the pipeline is represented in figure 1.9(a). In the right bottom corner is indicated the representation of a MAPMT and of a Trigger Generation board FPGA. In each FPGA $S_{i,k}$ represents the sum of pixels-on of the (i, k) MAPMT, i.e., the sum of the total number of pixels-on of the MAPMT located at the row i and column k. It is seen that each FPGA receives these values from the four MAPMT underlying it. For instance, the central FPGA receives, from the ProDAcqs, the values $S_{3,3}$, $S_{3,4}$, $S_{4,3}$ and $S_{4,4}$. In a second step the FPGAs communicate with their neighbours. Taking again the central FPGA, it receives from the top-left neighbour the value $S_{2,2}$, from the top neighbour the values $S_{2,3}$ and $S_{2,4}$ and from the left one the values $S_{3,2}$ and $S_{4,2}$. At the same time, this FPGA passes to their right, bottom and bottom-right the values $S_{3,4}$, $S_{4,3}$ and $S_{4,4}$. This process is represented in figure 1.9(b). In the end of this process the FPGA has information from a grid of 3×3 MAPMTS. In the third step of this trigger algorithm, also represented in the figure, the FPGA evaluates the total number of pixel-on for the four possible groups of 2×2 MAPMTs denoted by:

$$S_A = S_{3,3} + S_{3,4} + S_{4,3} + S_{4,4}$$

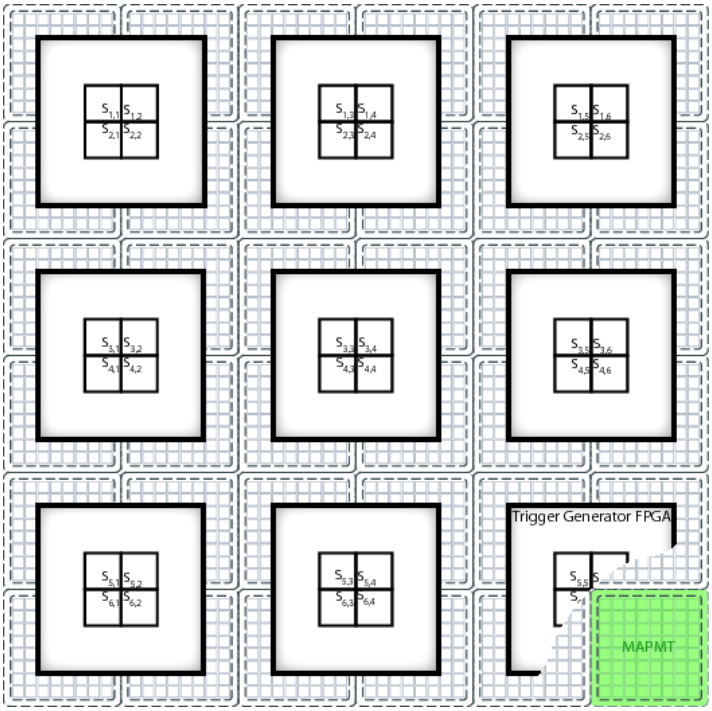

(a) first step of the pipeline

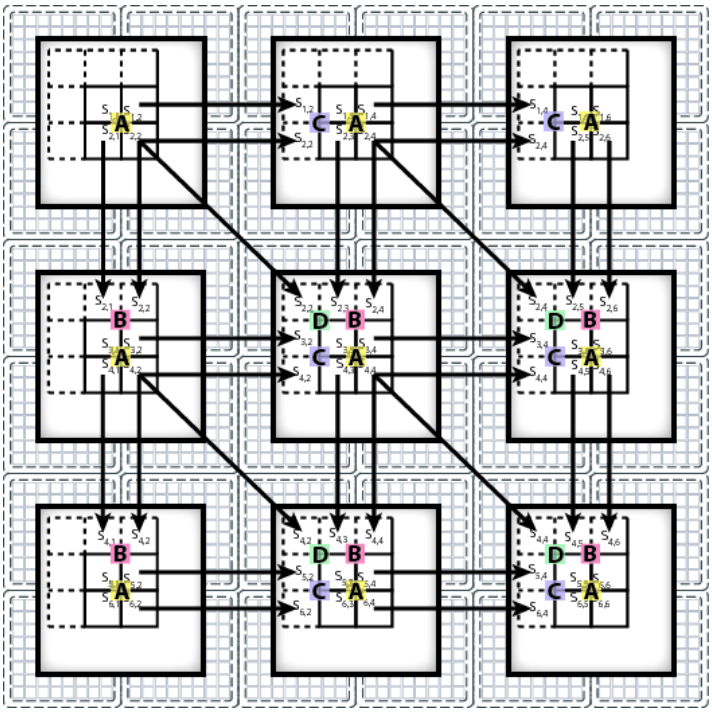

(b) second and third step of the pipeline

Figure 1.9: The second level trigger scheme.

$$S_B = S_{2,3} + S_{2,4} + S_{3,3} + S_{3,4}$$

$$S_C = S_{3,2} + S_{3,3} + S_{4,2} + S_{4,3}$$

$$S_D = S_{2,2} + S_{2,3} + S_{3,2} + S_{3,3}$$

If any of S_A, S_B, S_C or S_D is higher than the predefined threshold this FPGA issues a second level trigger signal.

The scheme exemplified is easily extended, for the whole focal surface, bearing in mind that the FPGAs in the edges do not communicate with some neighbours.

Third Trigger Level

In the third trigger level, the highest level in the GAW triggering system, the second level triggers are validated and a region of interest of the focal surface is defined to be read by the Data Acquisition system.

The third trigger level will be implemented on a FPGA that receives data from the second level trigger, i.e. from all the Trigger Generation Boards. Several modes can be implemented in this trigger level since the FPGA can be reprogrammed at any time.

In the basic mode a second level trigger in a GTU causes the whole focal surface to be read-out.

In order to reduce the bandwidth used, the third trigger level will have a mode that defines a Region Of Interest (ROI) to be read. The simplest algorithm is to define the ROI as the trigger-cells that produced a trigger and its neighbours. The number of neighbour trigger-cells to be read will be chosen to ensure that all the information belonging to an event is read. More sophisticated algorithms, including the rejection of specific noise patterns, may be implemented at this level.

In the final GAW configuration with three telescopes, a global event tag may be required. For this purpose it is foreseen that one of the telescopes can act as a central unit, receiving the third level trigger information from the other two telescopes. A temporal coincidence between the telescope triggers will be then performed and a global stamp will be issued and distributed.

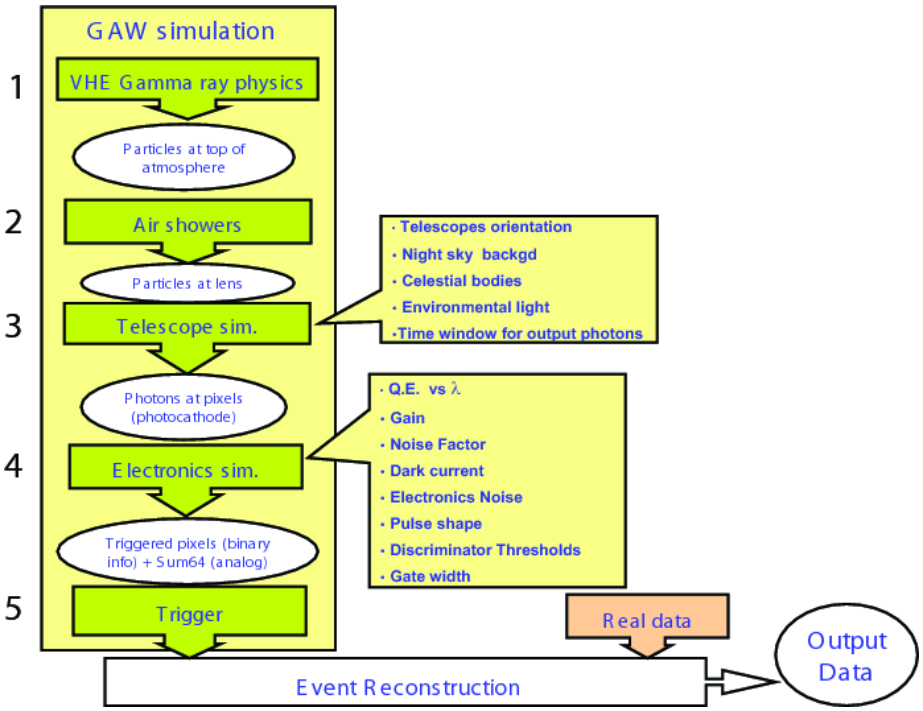

Figure 1.10: The GAW simulation Framework

1.2.5 Trigger expected performance

The triggering system performance is characterised by the capability to reject background events and by the efficiency for the selection of real events. To evaluate the trigger performance Monte Carlo simulations were developed at Palermo and at Lisboa.

At Palermo an IDL based simulation of the telescopes was used mainly to define the baseline design of the GAW telescopes. Background events were generated directly in IDL while gamma shower events were generated using CORSIKA [8] and the electronics and trigger were simulated afterwards in IDL. The specific details of such simulation are reported in [6]. A more exhaustive study on GAW performance [10] was made using CORSIKA and a custom program developed in Fortran that parametrises the lens response and simulates the Focal Surface and electronics.

At Lisboa, a global simulation framework for the GAW project was developed[12]. This framework defines the flow and the interfaces of the various programs and modules used to perform an end-to-end simulation of GAW. Figure 1.10 shows the structure of this framework. To assess the trigger performance the electronics and trigger simulation modules were implemented in the general framework using C++ and the ROOT toolkit. These modules allowed detailed cross-checks to be performed and provided an important tool for the study and development of trigger algorithms

and its implementation in the firmware.

Electronics simulation module

The electronics simulation module is a basic simulation of GAW electronics, including the noise generation due to the Night Sky Background and the simulation of the first trigger level. The focal surface, in this module, is composed of 80×80 pixels, corresponding to the focal surface of the first phase of the GAW project. The interface with GAW framework is performed through the file "Photons at pixels" generated by the Telescope Simulator which contains the information of each photon arriving at MAPMT the pixels. This information is read by the module and then a two-dimensional histogram is produced. Each bin of this histogram represents a pixel. Each photon is assigned to a bin, taking into account the PMT efficiency. A random number is uniformly generated between 0 and 1 and the photon is accepted if the value is lower than the efficiency factor. Thus each bin hold the number of collected photons. In this module the Night Sky Background (NSB) is introduced by generating for each pixel, and for each event, a random number following a Poisson distribution. The mean value of this distribution, $\langle B \rangle$, represents the average number of photo-electrons collected in that pixel due to the NSB and is chosen by the user, having a default value of 0.008 p.e./pixel/GTU.

For the purpose of this simulation it was assumed that the photomultiplier and the electronics do not introduce noise above the threshold of the first trigger level and that the first trigger level would operate with full efficiency for the detection of single photo-electrons. Thus if the number of photo-electrons in a pixel is greater than or equal to one the pixel is considered as a pixel-on. The output of this module consists of a pixel-on image of the focal surface.

A more detailed implementation of the first trigger level can be performed assigning a probability for the detection of the single photo-electron. Electronics noise, above the first trigger level threshold, can also be introduced at this level using the outlined scheme. It is planned to implement a more detailed description of the signal processing chain to be included in the general framework.

Second trigger level simulation module

The trigger module implements the simulation of the second level trigger. As described in section 1.2.2, this trigger level looks for an excess of pixels-on in trigger cells. These trigger cells are coded in the module, defining the pixels that constitute the cell. For each pixel-on image, a loop is performed in the trigger cells and, for

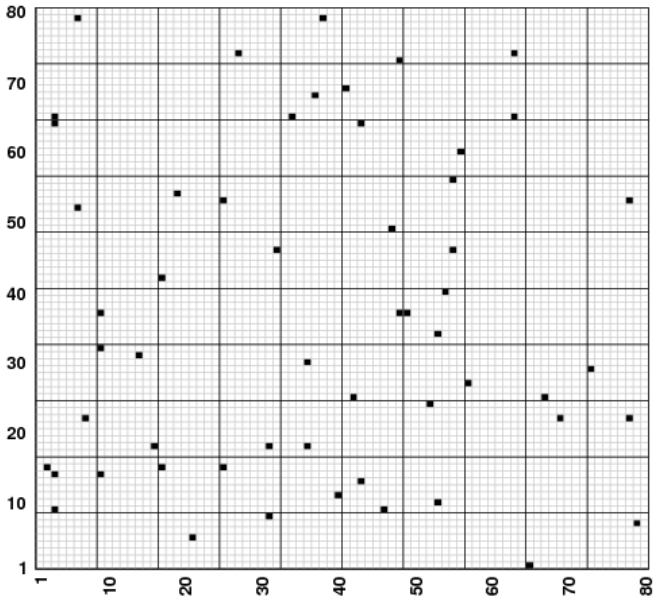

Figure 1.11: Image of GAW focal surface for a noise event. Each black square represents a pixel-on. The event was generated with a background level of $\langle B \rangle = 0.008$ pe/pixel/GTU

each one, the total number of pixels-on is calculated. The module outputs the maximum number of pixels-on in a trigger cell. A simple comparison with the second trigger level threshold can be performed afterwords to get a decision on the trigger of the simulated event.

Using the framework, and the developed modules, the rejection power of background and the efficiency for gamma events were studied and will be discussed in the following paragraphs.

Fake trigger rate estimation

Noise events were generated by simulating the pixel-on image formed in the Focal Surface due to the Night Sky Background. Figure 1.11 shows an image of the Focal Surface produced by a typical noise event produces for a background level of $\langle B \rangle = 0.008$ pe/pixel/GTU. In the image, the pixels-on are represented by black squares. Each event corresponds to the information present in the focal surface at each GTU of 10 ns. The output of the trigger simulator was used to increment a vector of the number of triggered events for several second trigger level thresholds. This vector holds thus the number of triggered events for the second trigger level

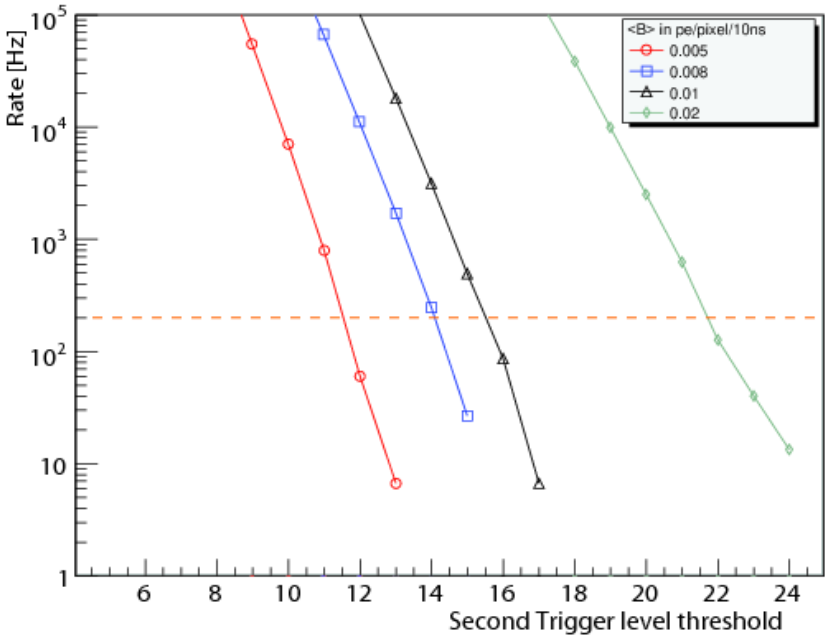

Figure 1.12: Fake trigger rate of a GAW telescope versus the second trigger level threshold. The different lines represent the fake trigger rate for several levels of background, $\langle B \rangle$ as indicated in the legend.

for each threshold level. The fake trigger rate at this level, η, is calculated as

$$\eta = \frac{\text{N. Triggered events}}{\text{N. generated events}} \cdot \frac{1}{\Delta t_{\text{GTU}}}$$

where Δt_{GTU} is the sampling period of the system.

The errors of the fake trigger rate, ε_η, were computed according to [15] as

$$\varepsilon_\eta = \sqrt{\frac{(k+1)(k+2)}{(n+2)(n+3)} - \frac{(k+1)^2}{(n+2)^2}} \cdot \frac{1}{\Delta t_{\text{GTU}}}$$

where k is the number of events that meet the trigger condition and n is the number of generated events.

The fake trigger rate as a function of the second trigger level threshold is shown in figure 1.12, for several levels of the background. The number of generated background events was 15×10^6. A reference value of 200 Hz of the fake trigger rate is indicated by an horizontal orange dashed line. This value is obtained in the GAW proposal [7] in the conditions of a background of $\langle B \rangle = 0.008$ pe/pixel/GTU and a second trigger level threshold of 14.

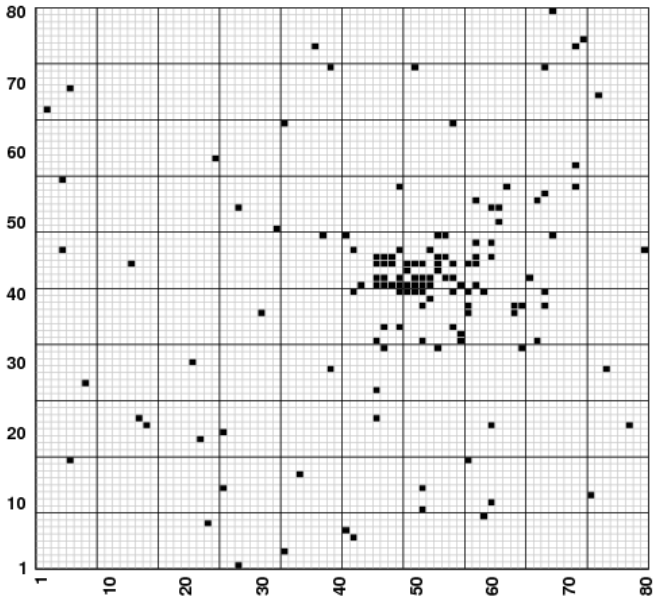

Figure 1.13: Image of a 1 TeV gamma event at the GAW Focal Surface

If the background level increases, e.g. in the presence of the moon in the sky, the fake trigger rate can be easily reduced by redefining the trigger threshold. From the figure it is seen that setting the second trigger level threshold at 22 a fake trigger rate lower than 200 Hz can be obtained even with a background as high as twice the typical one. Such background level can be found when a quarter moon is present in the sky at low zenith angles. However if the background increases too much the MAPMT looses its linearity and can even be damaged. An electronic protection is included in the front-end electronics to prevent damage to the PMT for very intense light levels.

Trigger efficiency estimation

The simulation framework was also used to study the trigger efficiency for different second trigger level thresholds. The CORSIKA program [8] version 6.617 was used to simulate gamma air showers, followed by the Telescope Simulator, developed in Geant4 [3, 2], the Electronics simulator and trigger simulator described before.

For this study, vertical gamma events were generated with the core of the air shower located at 100 m from the telescope, at fixed energies of 200, 300, 500, 700, 1000, 2000 and 3000 GeV. For each energy 100 events were generated. As an example, figure 1.13 shows a snapshot of the focal surface with a 1 TeV gamma

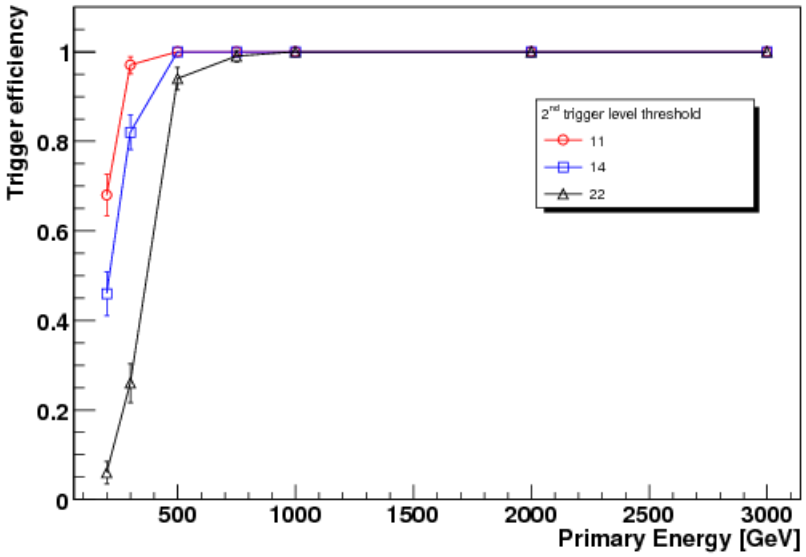

Figure 1.14: Trigger efficiency versus the shower primary energy for different trigger thresholds.

event, with each pixel-on indicated by a black square. For each event, the output of the trigger simulator was compared to three different thresholds of 11, 14 and 22. An efficiency was then calculated for each energy and each threshold as

$$\text{eff} = \frac{\text{N}^{\text{o}} \text{ triggered events}}{\text{N}^{\text{o}} \text{ generated events}}$$

with an error given by

$$\varepsilon_{\text{eff}} = \sqrt{\frac{(k+1)(k+2)}{(n+2)(n+3)} - \frac{(k+1)^2}{(n+2)^2}}$$

where k is the number of events that meet the trigger condition and n is the number of generated events. Figure 1.14 shows the obtained trigger efficiency as a function of the primary energy for each threshold. At low energies, the trigger efficiency is reduced with the increase on the trigger threshold, while energies above $\sim$ 1 TeV have a very high trigger efficiency regardless of the threshold set.

The light signal reaching the telescope varies with the distance to the shower core. Thus the maximum distance at which a shower can be detected, and hence the sensitivity of the telescope, varies with the energy and the trigger efficiency. An increase in the trigger threshold will reduce the sensitivity of the telescope. However the telescope can work with higher background levels, with acceptable sensitivity

for high energetic showers, thus increasing the total exposure.

The estimation of the effective area with the energy and trigger threshold will require a large sample of showers at different energies and distances

1.2.6 System firmware

The system firmware for a great part of the acquisition electronics is a responsibility of the LIP group. Namely, LIP is responsible for the development of the firmware for ProDAcq boards and for the Trigger Generation boards.

A test bench to test the ProDAcq is installed in the e-CRLab that consists on a ProDAcq board, two interface boards and test and measuring equipment. An interface board, named ProDAcq-Excite, allows the ProDAcq signal inputs to be coupled to a signal generator or to an external FPGA. These external sources allow the output from a FEBrick unit to be emulated. The signal generators available allow four independent input signals to be produced. When coupled to a FPGA development kit it is possible to generate all the 64 input signals of the ProDAcq, allowing all possible configuration of the input signals to be tested. However, the output of the FPGA is digital and the shape and timing of the signals cannot be controlled as well as with the signal generators. Another interface board, named LIP-CTRIG, is used for power supply, programming interface and to connect the trigger and control bus to external equipment. The trigger information can be seen in a logic analyser or it can be coupled to a FPGA development kit which is also used to input data in the control and trigger bus. Although the use of an FPGA to interface the board adds extra flexibility, the performance tests need to be performed using the logic analyser to assure correct time measurements. In particular the logic analyser available is capable of performing timing measurement with sub-nanosecond accuracy.

Several firmware modules for the ProDAcq have already been developed, mainly for functional tests of the board. The ProDAcq board can operate in two distinct modes. The firmware takes that into account and the user can choose at run time the acquisition mode. Additionally every parameter that the firmware uses will also be programmable by the user.

In the first mode, used mainly for testing, the ProDAcq counts how many times each pixel has been activated. This count is performed with a sampling period that corresponds to the normal acquisition frequency for a pre-determined time interval (of the order of seconds). In this way the light flux at each pixel can be evaluated. This mode can be used to, e. g., estimate the background level or, if the telescope

is pointed to a star, to evaluate the optical spot produced in the Focal Surface.

In the second mode, the acquisition mode, the ProDAcq receives data from the FEBrick and saves it in a ring memory. At the same time it counts the number of pixels-on and outputs this value to the trigger bus. This algorithm is part of the pipeline scheme of the trigger system and needs to be performed each sampling period. Moreover the algorithm must always take the same time so that a reference to stored data is available. When a trigger strobe is received from the Trigger Generation boards, the ProDAcq saves the corresponding data that will be read through the control bus. The board firmware also comprises the implementation of the control and read-out protocol that is yet to be defined.

The firmware of the Trigger Generation board implements the trigger algorithm described before. In each sampling period, the board receives the number of pixels-on from four ProDAcqs. In a following step the board will exchange data with its neighbours and then applies the majority trigger algorithm. When the trigger condition is met the trigger generation board issues a trigger strobe to the relevant ProDAcqs. In the baseline design the ligh-guides are composed by 64 segments, one per pixel. Its fabrication and assembling showed to be a challenge. Thus, other options were studied, namely the option of reducing the number of segments by a factor 4. This fact has delayed the development of the Trigger Generation boards as the pitch between PMTs depends on the final design of the light-guides. The trigger firmware tests will start as soon as these boards become available.

Bibliography

[1] Photon counting using photomultilier tubes, *Tech. rep.*, Hamamatsu, 2005.

[2] Agostinelli, S., et al., Geant4-a simulation toolkit, *Nuclear Instruments & Methods in Physics Research Section A-Accelerators Spectrometers Detectors and Associated Equipment*, *506*, 250–303, 2003.

[3] Allison, J., et al., Geant4 developments and applications, *IEEE Transactions on Nuclear Science*, *53*, 270–278, 2006.

[4] Assis, P., How to select UHECR in EUSO: The trigger system, in *New worlds in astroparticle physics - Proceedings of the fifth international workshop*, pp. 120–123, World Scientific, 2005.

[5] Catalano, O., EUSO trigger - method and operational criteria, *Tech. Rep. EUSO-TEO-REP-002*, EUSO, 2003.

[6] Catalano, O., M. C. Maccarone, and B. Sacco, Single photon counting approach for imaging atmospheric cherenkov telescopes, *Astroparticle Physics*, *29*, 104–116, 2008.

[7] GAW collaboration, Gamma air watch (gaw) - concept design and science case, 2005.

[8] Heck, D., J. Knapp, J. Capdevielle, G. Schatz, and T. Thouw, CORSIKA: A Monte Carlo code to simulate extensive air showers, *Tech. Rep. FZKA 6019*, Forschungszentrum Karlsruhe, 1998.

[9] Knoll, G. F., *Radiation Detection and Measurement*, John Wiley and Sons, Inc., 2000.

[10] Maccarone, M. C., Study of the gaw expected performance. part 1: Analysis at trigger level., *Tech. Rep. GAW_EVE_0004_061127*, IASF-Pa/INAF, 2006.

[11] Pallavicini, M., and A. Thea, Esaf user guide, *Tech. Rep. EUSO-SDA-REP-014-1*, EUSO, 2004.

[12] Pimenta, M., A. Pina, and B. Tomé, GAW simulation framework, *Tech. Rep. GAW_SIM_0008*, GAW, 2007.

[13] Thea, A., Osservazione di radiazione cosmica di altissima energia dallo spazio, Ph.D. thesis, Università degli studi di Genova, 2006, (in English).

[14] Thea, A., et al., The EUSO simulation and analysis framework, in *Proceedings of the 29th International Cosmic Ray Conference Pune*, vol. 8, pp. 133–136, 2005.

[15] Ullrich, T., and Z. Xu, Treatment of errors in efficiency calculations, *arXiv:physics/0701199v1*, 2007.